Effect of Nano-silica Deposition on Cellulose Fibers on the Initial Hydration of the Portland Cement

Joabel Raabe,[a,*] Laryssa Paz dos Santos,[a] Cláudio Henrique Soares Del Menezzi,[a] and Gustavo Henrique Denzin Tonoli [b]

The surface modification of cellulose fibers was studied, and its influence on the initial hydration of fiber-cement mixtures was evaluated. The fiber modification was conducted through deposition of nano-silica on their surface *via* the sol-gel method. The fibers were characterized by scanning electron microscopy, energy dispersive spectroscopy, X-ray diffraction, and the Brunauer-Emmett-Teller method to determine their porosity and specific surface area. The inhibition index (II) was determined in order to evaluate the effect of fibers at the initial hydration of the Portland cement. Modified fibers (MF) presented a homogeneous surface coating formed by spherical nano-silica. The crystallinity index of the fibers was reduced 15% and the specific surface area, volume, and pore diameter increased 209%, 134%, and 10%, respectively, after modification. Regarding the initial hydration, the results showed that the nano-silica present on the surface of the MF slightly accelerated the process of hardening and did not inhibit the hydration of the cement paste (without limestone and additives). The inhibition index of the composites was impaired when limestone (30%) and additives (2%) were added as partial replacement of cement, as well as when the water:cement ratio increased, retarding the initial hydration of the cement.

Keywords: Composites; Cement; Cellulose Pulp; Modified Fibers; Inhibition Index

Contact information: a: Department of Forest Engineering, University of Brasilia, Campus Darcy Ribeiro, Faculty of Technology, Asa Norte, 70910-900, Brasília, DF, Brazil; b: Department of Forest Science, Federal University of Lavras, P.O. Box 3037, 37200-000 Lavras, MG, Brazil;
** Corresponding author: joabeljr@hotmail.com*

INTRODUCTION

The procurement of durable, cheap, and environmentally friendly materials that are not dangerous to human health is one of the manufacturer's main interests that drives several sectors of the construction industry to provide alternatives. Fiber-cement fits in this context, being a composite that is widely used in civil construction, namely roofing tiles, claddings, panels, and water tanks. Fibers available commercially for composites are metallic (steel fibers), synthetic fibers (mainly acrylic, aramid, carbon, nylon, polyester, polyethylene and polyvinyl-alcohol), and natural (sisal, cellulose pulp, others).

Steel fibers provide strength to fiber-cement composites because of their high elastic modulus, high strength, and relatively low deformation capability; by contrast, the improvement of the ductility and post-cracking capacity of the fiber-cement with steel fibers is limited (Soufeiani *et al.* 2016). In addition, the high-cost steel fibers are abrasive and corrosive in nature. Synthetic fibers, due to their properties (high tensile strength, elasticity modulus, ultimate strain, and low specific gravity) have been shown to be durable under many normal and harsh conditions with good bonding with cement and do not cause

health problems (Khan *et al.* 2017). However, synthetic fibers demand a lot of energy for production and often make them not environmentally friendly, besides being basically non-renewable material.

Natural fibers such as sisal, jute, cotton, flax, hemp, kenaf, wood fibers (cellulose pulp), and so on have already been considered as potential alternatives to traditional fibers given the advantages such as renewable and readily available material, low density and non-abrasive materials, and the fact that they can be extracted at low energy consumption and low cost (Silva *et al.* 2008; Santos *et al.* 2015). Cement-based composites reinforced with natural fibers exhibit improved toughness, ductility, flexural capacity, and crack resistance compared with non-fiber-reinforced cement-based materials. The major advantage of fiber reinforcement is the post-cracking behavior, whose fibers bridge the matrix cracks and transfer the applied load (Ardanuy *et al.* 2015). The interfacial interaction of the fibers with the matrix is often hampered by high dimensional instability of the cellulosic fiber due to their hydrophilic character. The cellulosic fiber absorbs Ca-rich hydration products of the cement, leading fibers to the so called mineralization process and causing the fiber to become stiffer. The high alkalinity (pH around 13) of the hydrated cement paste and the massive presence of $Ca(OH)_2$ in the pore solution dissolves lignin and hemicelluloses of the fibers, degrades the cellulose molecular chains and reduces its degree of polymerization, weakens the cell wall by means of crystallization of $Ca(OH)_2$ in the fiber cavities, which leads to a decrease in the flexibility and technical strength of the fibers (Gram 1983; Singh 1985; Tolêdo Filho *et al.* 2000; Wei and Meyer 2015). Thus, when cellulose fibers are exposed to a highly alkaline environment such as Portland cement composites they are subject to deterioration and loss of their ductility, which seriously diminishes durability and can lead to premature composite failure (Tonoli *et al.* 2013a; Pizzol *et al.* 2014; Tonoli *et al.* 2016). Therefore, the degradation of natural fibers in cement matrixes has been a central issue that must be improved in order to turn viable the widespread application of natural fiber in various composites (Wei and Meyer 2017).

There are several studies in the literature that report the advantages of the used pulp cellulose as reinforcement in fiber cement composites. However, the question of low durability has not yet been overcome. Therefore, in order to mitigate the degradation of naturally occurring fibers in the cement matrix and improve the durability of the cementitious composites, pretreated (modified) cellulose pulp fibers may be an alternative. However, the use of cellulose pulp fibers in fiber-cement is still a challenge in terms of compatibility between the reinforcement and matrix, and fiber durability in an alkaline medium, especially when exposed to aggressive environmental conditions (Agopyan *et al.* 2005).

A strategy for improving the durability of cement composites consists in the modification fibers of cellulose pulp by refining the pulps, with hornification treatments or chemical surface treatments (Ardanuy *et al.* 2015). Several approaches have been reported on the use of chemical surface treatments on cellulose fibers to reduce their hydrophilic character and improve their adhesion to the matrix (Belgacem and Gandini 2005; Onuaguluchi and Banthia 2016). Isocianate-treated (Tonoli *et al*. 2013b), latex polymer film and a pozzolan layer (Silva *et al.* 2017) and silane-treated fibers (Pehanich *el al.* 2004; Bilba and Arsene 2008; Tonoli *et al.* 2009, 2013a; Mendes *et al.* 2015) were previously tested in fiber-cements showing several contributions to physical, mechanical, and durability performance of the composites. They were all based on exploiting the reactive hydroxyl functions of the fiber surface through different chemical procedures. The blocking of chemical pathways reduces the number of reactive hydroxyl groups

concomitant with the formation of bonds between the cellulose fibers and the cementitious matrix (Tonoli *et al.* 2009). In addition, pretreatments or modifications of the cellulose fibers aim to protect the amorphous regions of the cellulose, where the vulnerabilities are found and prone to degradation of the fibers in the alkaline medium. In these regions, in addition to the repeated glucose units, the cellulose molecules have a non-reducing (C1-OH) and a reducing (C4-OH) extremity. The alkaline degradation of the cellulose depends mainly on the reducing end in amorphous regions (Wei 2018).

Therefore, the incorporation of inorganic (nanoscale) components on the surface of cellulose pulp fibers *via* the sol-gel method may be a promising alternative because it results in the formation of a new class of reinforcement that combines the main characteristics of inorganic and organic materials. The deposition of nano-silica (SiO_2) on the surface of cellulose pulp fibers through the sol-gel method allows a homogeneous coating and decrease of water adsorption capacity of the fibers (Pinto *et al.* 2008; Raabe *et al.* 2014). This method promotes an improved interface between the fiber and the cementitious matrix and acts on hydration of the cement, due to the reduction of competition by water, and consequently reduces the mineralization of the fibers in an alkaline medium. This research has provided considerable advances in the understanding of fiber-cement using vegetable fibers. However, the study of vegetal fiber's effect in the initial hydration of the cement is rarely realized and has not been sufficiently explored. Effective interaction between matrix and fiber can be considered primordial, which makes initial hydration an important topic for evaluation because it may assist for optimization of the curing process, or increase of productivity and performance. Therefore, the objective of this study is to evaluate the surface modification of cellulose fibers with nano-silica and their influence on the initial hydration of the fiber-cement composites.

EXPERIMENTAL

Materials

Bleached eucalyptus cellulose kraft pulp was supplied by Eldorado Brazil Cellulose (Três Lagoas, MS, Brazil). These commercial cellulose pulp fibers presented the following properties provided by the manufacturer: fiber length of approximately 650.0 μm, fiber diameter of approximately 16.6 μm, aspect ratio of approximately 39.1, and an approximate 90.9% ISO whiteness. Additionally, 91.1% *alfa* cellulose, approximately 0.11% insoluble in HCl, approximately 0.09% extractives in acetone, and approximately 0.30% ash. The fibers had a water retention index of approximately 152% and apparent density of approximately 800 kg/m^3.

The chemical agents used for modification of the fibers were: tetraethyl orthosilicate ($C_8H_{20}O_4Si$; TEOS, 98%) supplied by Merck Millipore Corporation (Barueri, SP, Brazil) as the inorganic precursor for the synthesis of SiO_2; ammonium hydroxide (NH_4OH; 30% to 32% $v.v^{-1}$) as the synthesis catalyst; and ethanol (CH_3CH_2OH; 95%) provided by Vetec Quimica Fina Ltda. (Duque de Caxias, RJ, Brazil) as the solvent.

The cement-based matrix was formed by Portland cement type V of high initial resistance and resistant to sulphates (CP V-ARI RS) according to the ABNT NBR 5737 (1992) standard. The material was supplied by CIPLAN cements (Sobradinho, DF, Brazil) and it was chosen because of its thinner particle size and great reactivity. Ground agricultural limestone was used as filler for the partial substitution of Portland cement for cost reduction (Bezerra *et al.* 2006) (SN Concreto Ltda., Ijaci, MG, Brazil). The additives

used in the experiment were hydroxypropyl methylcellulose (HPMC) with a viscosity between 60000 cP and 70000 cP (Aditex Ltda., São Paulo, SP, Brazil) and polyether carboxylic acid (ADVA 175) with specific mass of 1.05 kg/m^3 to 1.09 kg/m^3 and pH between 4.0 and 6.0 (Grace Brasil Ltda., Sorocaba, SP, Brazil). Cellulose esters (which includes HPMC) generate excellent thickening effect due to the increase of viscosity and water retention capacity (Brumaud *et al.* 2013). With regard to cement hydration, HPMC can significantly delay the hydration induction period and the acceleration period of cement pastes (Pourchez *et al.* 2006). The superplasticizers (which includes ADVA) are used to improve the workability of concrete in practice, and are becoming indispensable components in concrete to modify the workability of fresh concrete and/or to reduce the water demand (Zhang *et al.* 2015).

Methods

Modification of cellulose pulp fibers and characterization

The modification of the cellulose pulp fibers was accomplished by the deposition of silica (SiO_2) nanoparticles on the surface of the fibers, by means of the sol-gel process, as reported by Raabe *et al.* (2014). The modification process consisted of the previous dispersion of cellulose pulp fibers in water that was then immersed in a solution composed of ethanol (85.0%), water (9.0%), ammonium hydroxide (1.5%), and tetraethyl orthosilicate (TEOS) (4.5%). The fibers were added to the solution at a ratio of 1:100 (g.mL^{-1}). This modification process was performed under ambient conditions in subsequent steps. First, the previously dispersed fibers were added to the solution containing ethanol, water, and ammonium hydroxide, and mixed under constant and moderate stirring (500 rpm) for 30 min. Next, under constant stirring, the nano-silica precursor (TEOS) was slowly added (dropwise). The mixture was stirred for 18 h, which is sufficient time for formation and coating of the fibers with nano-silica (Raabe *et al.* 2014). Lastly, the fibers were washed with distilled water until complete removal of the reaction solution and oven-dried at 70 °C ± 5 °C.

The fibers were characterized for their surface morphology, microstructure, surface area, and porosity before and after modification. The surface morphology of the fibers was evaluated by scanning electron microscopy (SEM; model JSM-7001F, JOEL, Tokyo, Japan), operated at a power of 15 kV, using a secondary electron (SE) detector. Samples of unmodified (UMF) and modified (MF) fibers were previously coated with a thin layer of gold (Bal-Tec, model SCD-050, Scotia, NY, USA). An energy dispersive spectroscopy (EDS) system (JOEL, Tokyo, Japan) was used to detect and quantify the presence of silicon on the surface of the fibers. To detect the degree of coating of the fibers by the modification process, 16 random EDS readings were performed for each type of fiber (UMF and MF).

X-ray diffraction (XRD) was used to evaluate how much the modification may have been able to alter the degree of crystallinity of the UMF in comparison to the MF. A Bruker diffractometer (model D8 Discover, Atibaia, SP, Brazil) with employed radiation of Cu-Kα was used for this purpose. The measurement conditions were 40 kV with a scanning speed of 2°.min^{-1} for values of 2θ between 10° and 35°. The crystallinity index (CI) was calculated according to Eq. 1, adapted from Ford *et al*. (2010),

$$CI\ (\%) = \left[\left(\frac{I_{200} - I_{AM}}{I_{200}}\right)\ x\ 100\right] \quad (1)$$

where *CI* is the crystallinity index (%), I_{200} is the maximum intensity diffracted by crystalline cellulose ($2\theta \cong 22$), and I_{AM} is the intensity of diffraction of the amorphous portion of cellulose ($2\theta \cong 18^{o}$).

The surface area and porosity of the fibers were estimated by adsorption/desorption isotherms of nitrogen gas (N_2) at 77 K using the volumetric gas adsorption analyzer Quantachrome NovaWin (NovaWin, version 10.01, Boynton Beach, FL, USA). Based on the curves generated by the pressure variation of the adsorption and desorption isotherms, the specific surface area was estimated by the Brunauer-Emmett-Teller (BET) method. The analysis of the isotherms obtained were used to determine the diameter and the mean volume of the pores.

The effect of fibers at initial cement hydration

The effect of fibers (modified or not) at the initial cement hydration of the fiber-cement composites (UMF and MF) was evaluated, within the first 48 h after mixing the components. The samples were maintained in closed containers and two matrix formulations were used. For better understanding of the effects of the fibers on the initial hydration of the two matrices, the evaluation was divided into two parts (part 1 and part 2). Fiber-cement composites were prepared and their respective compositions are described in Table 1.

Table 1. Composition of the Fiber-cement Composites

Treatment		Cement Matrix (g)				Fibers (g)	
		Cement	Limestone	HPMC	ADVA	MF	UMF
Part 1	Control	100.0	-	-	-	-	-
	C + UMF	100.0	-	-	-	-	7.5
	C + MF	100.0	-	-	-	7.5	-
Part 2	Control'	100.0	-	-	-	-	-
	C_{LA}	68.0	30.0	1.0	1.0	-	-
	C_{LA} + UMF	68.0	30.0	1.0	1.0	-	7.5
	C_{LA} + MF	68.0	30.0	1.0	1.0	7.5	-
C = Cement; UMF = Unmodified Fiber; MF = Modified Fiber; L = Limestone; A = additions (HPMC and ADVA)							

The matrix:fibers ratio was established as described in Weatherwax and Tarkow (1964) and Hofstrand *et al*. (1984), and the water:cement matrix ratio was 0.45:1 for the control and C_{LA} (cement, limestone, and additions) samples. However, for mixtures that contained fibers, the ratio was increased to 0.68:1 as a result of the high water absorption capacity of the fibers and in order to improve the homogeneity of the mixture.

The components were mixed with a vertical axis mechanical stirrer (approximately 500 rpm) (model RW 20, IKA, Staufen im Breisgau, Germany). First, the fibers were dispersed in distilled water (ratio of 1 g of fibers for 100 mL of water), the excess water was withdrawn, and the amount of water retained in the fibers was determined by the difference between the wet mass and the dry mass of the fibers. The water content retained in the fibers was considered as part of the water of the mixture. Subsequently, the fibers were mixed with the other components until complete homogenization, in the following order: (I) previously dispersed fibers; (II) cement, limestone, and HPMC (when appropriate), previously manually mixed; and (III) distilled water and ADVA (when appropriate). The interval between adding the components of stages I, II, and III was approximately 2 min.

The mixture was then placed in polyvinyl chloride (PVC) containers, and a "K" type thermocouple cable was inserted into the center of each mixture (Fig. 1a). Subsequently, each PVC container was packaged in its respective heat containers that were insulated from each other and stored in a thermal box (Fig. 1b). The thermocouple cables were connected to a signal receiver (ICEL datalogger, model TD-890; Icel Manaus, Manaus, Amazonas, Brazil) to perform readings and record temperature data at 2-min intervals for a period of 48 h. The tests were performed separately in series, each series corresponding to a treatment and composed of three replicates. A reference sample (control = cement + water) served as basis for the evaluation and analysis of the results.

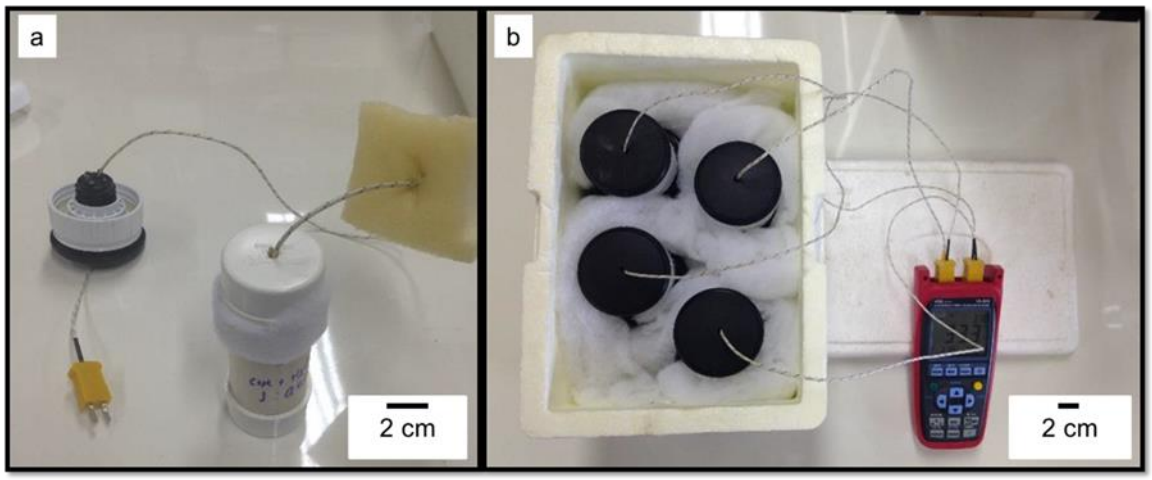

Fig. 1. Apparatus for evaluation of the effect of the fibers (MF and UMF) at the initial hydration of fiber-cement.

The inhibition index (II) was calculated according to Eq. 2, as developed by Weatherwax and Tarkow (1964) and Hofstrand *et al*. (1984),

$$II\ (\%) = \left[\frac{(T_{cim} - T_m)}{T_{cim}} . \frac{(H_m - H_{cim})}{H_{cim}} . \frac{(S_{cim} - S_m)}{S_{cim}}\right] x\ 100 \qquad (2)$$

where T_{cim} is the maximum temperature of the cement/water mixture (°C), T_m is the maximum temperature of the fiber/cement/water mixture (°C), H_m is the time to reach the maximum temperature in the fiber/cement/water matrix mixture (h), H_{cim} is the time to reach the maximum temperature in the cement/water mixture (h), S_{cim} is the maximum temperature increase of the curve in the cement/water mixture (°C/h), and S_m is the maximum temperature increment of the curve in the fiber/cement/water matrix mixture (°C/h).

The effect of the inhibition of the fibers at the initial hydration of the fiber-cement was classified based on the inhibition index (II) according to Table 2.

Table 2. Classification of the Lignocellulosic Material According to the Inhibition Index (Okino *et al.* 2004)

Inhibition Index - *II* (%)	Classification
II ≤ 10	Low inhibition
10 < *II* ≤ 50	Mean inhibition
50 < *II* ≤ 100	High inhibition
II > 100	Extreme inhibition

Analysis of results

A statistical analysis for the fiber characterization results and the effect of the fibers at the initial hydration (inhibition index) followed the completely randomized experimental design. An analysis of variance (ANOVA) and Tukey test, for the comparison of the means with 5% of probability in cases of rejection of the null hypothesis, were conducted with ASSISTAT software (Federal University of Campina Grande, version 7.7, Campina Grande, Paraiba, Brazil).

RESULTS AND DISCUSSION

Characterization of the Fibers

Macroscopic and SEM images of the UMF and MF were captured to verify the changes on the surface morphology of the fibers after the modification process, as shown in Fig. 2.

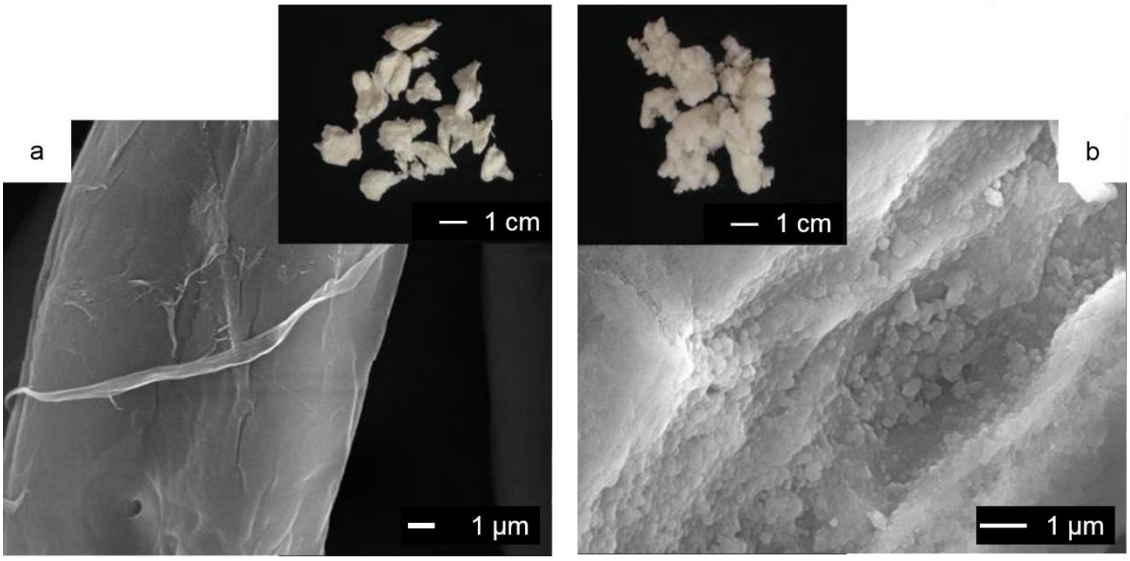

Fig. 2. Typical SEM images of the surface of UMF (a), and of MF (b), with respective macroscopic images (inset) of fiber agglomerates

The surface of modified fibers (Fig. 2b) was noticeably rougher compared to the surface of the unmodified fibers (Fig. 2a). The difference was due to the presence of spherical silica (SiO_2) particles and nanoparticles on the surface of the MF. Rough surfaces allowed for greater interfacial interaction between the reinforcement and matrix, which led to higher mechanical bond strength. Silica deposition is due to the sol-gel reactions by the hydrolysis of the TEOS precursor and subsequent silica condensation (Xie *et al.* 2009) on the cellulose fiber surface. The silanol reactive groups from the TEOS react with the free hydroxyl groups of cellulose, which forms the Si-O-Si bond (Pinto *et al.* 2008; Ashori *et al.* 2012). The interaction between the fiber surface and the silica particles, guaranteed by strong chemical bonds (covalent bonds) is hard to disrupt (Hussain *et al.* 2018). The spherical format is due to the alkaline middle of the sol-gel reaction, typical of hybrids synthesized in the presence of a basic catalyst, which in the present case was ammonium hydroxide (Benvenutti *et al.* 2009).

The macroscopic images of Figs. 2a and 2b (inset) show UMF and MF, respectively. There was clearly larger agglomeration of fiber and lower fiber volume for UMF in relation to the MF. These differences are related to the decrease of free hydroxyls available on the surface of the fibers when nano-silica are deposited (Raabe *et al*. 2015). Free hydroxyls increase the agglomeration (interlacing) between fibers upon drying. Additionally, the MF tended to present better dispersion in the cementitious matrix and consequently may have allowed greater reinforcement efficiency and performance when external forces were transferred to the composite.

The fibers were also analyzed by EDS to semi-quantify the presence of the silicon element on the surface of the modified fibers. Table 3 presents the mean content values of the main elements present on the surface of the fibers (UMF and MF) determined by EDS analysis. Clearly, there was a significant increase of Si concentration and a significant decrease of C and O concentration on the surface of the MF in relation to UMF. This was due to the deposition of nano-silica on the surface of the fibers as detected in different points of different fibers.

Table 3. Mean and Standard Deviation Values of the Content of Carbon (C), Oxygen (O), and Silicon (Si) Elements in UMF and MF*

Fiber Type	C	O	Si
	% Based on Mass		
UMF	43 ± 4 a	57 ± 3 a	0.6 ± 0.6 b
MF	24 ± 10 b	45 ± 11 b	31 ± 9 a
*Means followed by the same letter within the same column do not differ statistically from each other by the Tukey test at the 5% level of significance			

The typical X-ray diffractograms of the cellulose fibers (UMF and MF) and their respective CI values are shown in Fig. 3.

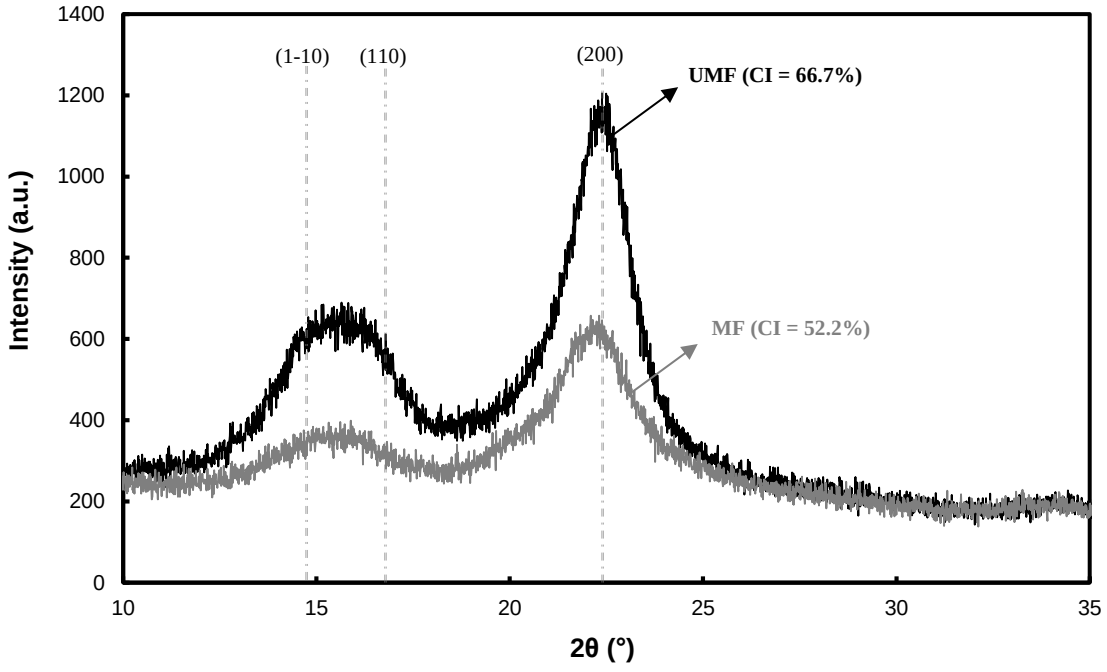

Fig. 3. Typical X-ray diffractograms of UMF and MF with respective CI values

The XRD patterns of the fibers had an amorphous broad hump and crystalline peaks typical of semicrystalline materials. The XRD of the fibers (Fig. 3) showed similar structures to cellulose Iβ with preferred orientation of the crystallites along the fiber axis (French 2014). This orientation became clear due to shoulder peak at 2θ = 20.5°, which was not evident in either of the curves (French 2014). The fibers studied exhibited a sharp peak near 2θ = 22.6°, which was assigned to the (200) lattice plane of cellulose I. The peak of the plane (200) in the UMF was sharper than for MF, which is indicative of greater crystallinity, at least in relation to the (200) plane (Cao and Tan 2005). The two overlapping weaker diffraction peaks at 2θ = 14.8° and 2θ = 16.3° are assigned to the (1-10) and (110) lattice planes of cellulose I (Klemm *et al.* 2005; Besbes *et al.* 2011).

The deposition of nano-silica decreased the CI of the MF in approximately 15% in relation to the UMF. This change was observed by the difference of peak intensity in (200), (1-10), and (110) planes of the studied fibers (Fig. 3). Nano-silica synthesized *via* the sol-gel method, using TEOS as a precursor, were amorphous and therefore contributed to the decrease of the relative crystallinity of the fibers when they were chemically bound to the fiber surface. Although nanoparticles interfered with the CI, the internal microstructure of the MF's cell wall in relation to the UMF did not appear to have been altered. Concomitantly, the modification allowed the formation of a new hybrid material (organic-inorganic) with different properties, as previously reported by others (Pinto *et al*. 2008; Ashori *et al*. 2012; Raabe *et al*. 2014).

As previously discussed, the surface morphology of MF was greatly changed, presenting a surface covered with nano-silica that made them rougher and altered the initial porosity and surface area of the cellulose pulp fibers. To confirm the change in porosity, the fibers were subjected to N_2 adsorption/desorption under controlled pressure, and the isotherms are presented in Fig. 4.

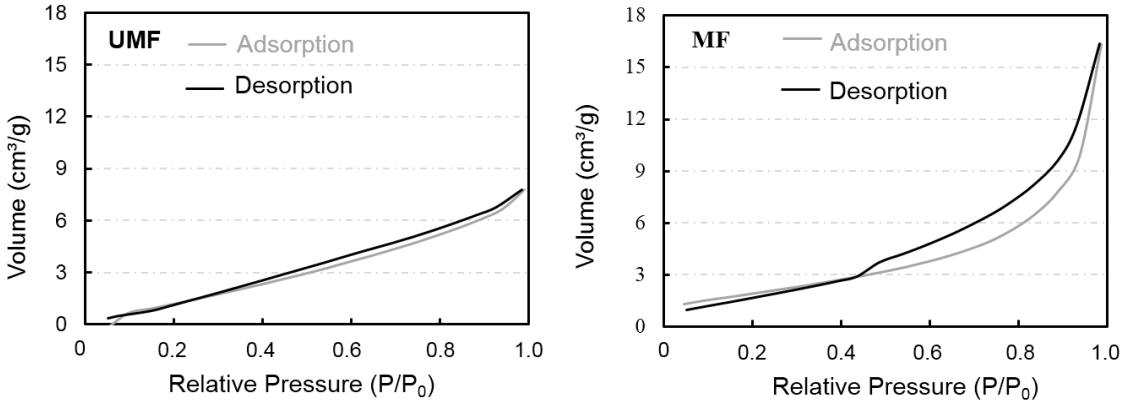

Fig. 4. Typical N_2 adsorption and desorption isotherms for UMF and MF

The hysteresis was observed for the two fiber conditions (UMF and MF), characterized by two distinct branches, similar to the IV-type characteristic of mesopore-containing solids (Cessa *et al.* 2009). Iftekhar *et al.* (2017) evaluated adsorption/desorption isotherms of nanocomposites formed by cellulose and silica and observed the typical IV-type (for mesoporous materials) classified as H2 with a wide hysteresis loop, similar to that shown in Fig. 4 for MF. This behavior is often reported for mesoporous solids composed of particle agglomerates, generating crack-shaped apertures (Sing *et al.* 1985). Possibly,

such a characteristic was associated with the deposition and agglomeration of the nano-silica on the surface of the fibers, as seen in Fig. 2b.

The narrow and inclined curves in the UMF isotherm (Fig. 4) indicated small pore size distribution (Pena *et al.* 2008). In the case of MF, there was a larger distribution of pores with the presence of macropores, evident by the essentially vertical rise near pressures of $P/P_0 = 1$ (Sing *et al.* 1985). Another consequence of the fiber modification was the significant increase (approximately 209%) of the surface area of the fibers. In addition, MF also presented an increase of volume (approximately 134%) and pore diameter (approximately 10%) in relation to UMF (Table 4).

Table 4. Means and standard deviation values of Surface Area, Volume, and Pore Diameter for UMF and MF*****

Fiber Type	Surface Area (m^2/g)	Volume** (cm^3/g)	Pore Diameter** (Å)
UMF	2.3 ± 1.6 b	0.011 ± 0.002 b	33.6 ± 0.1 b
MF	7.1 ± 0.3 a	0.025 ± 0.001 a	37.1 ± 0.1 a

* Means followed by the same letter within the same column do not differ statistically from each other by the Tukey test at the 5% level of significance;
** Determined by the method proposed by Dollimore and Heal (DH), because the fibers have mesopores with cylindrical or slit geometry (Farias 2012)

The specific surface area is limited by the external surface of the solid material and the internal surface produced by its porosity (Santana *et al.* 2012). The specific surface area is inversely proportional to the mean pore diameter, *i.e.*, a large specific surface indicates the presence of small pores while small values are characteristic of macroporous and non-porous materials (Svarovsky 1987; Lowell and Shields 1991). This occurs when the pore volume remains constant, because when the pore volume increases significantly, the specific surface area also increases, even with increasing pore diameter (Table 4). Therefore, MF may favor the mechanical interaction with the matrix due to the higher surface area, volume and pore diameter.

The tendency of more porous materials is to increase their moisture adsorption capacity. However, despite the surface area, the pore volume and pore diameter of the fibers increased after their modification. Previous studies done by Pinto *et al*. (2008) and Raabe *et al.* (2014) reported a decrease in moisture adsorption capacity of the fibers of cellulose pulp after silica deposition *via* the sol-gel method. This more hydrophobic character may have decreased the water competition between the matrix and the fibers, favored the initial hydration, and promoted better interaction of the fibers with the cementitious matrix. In addition, the modification may have prevented the weakening of the fibers caused by the mineralization process (migration of the calcium hydroxide to the fibers' cavities in a highly alkaline aqueous solution) describe by Tonoli *et al.* (2016).

The resulting material of modification by the deposition of nano-silica in fibers of cellulose pulp, although it has undergone a chemical process, its relative cost can be considered low, because the sol-gel process is considered low cost, besides presenting higher productivity and environmentally benign when compared to other instrumental and physical methods (Singh *et al.* 2014). This modification process still requires optimization for the different conditions of the pulp fibers. Modification costs were not evaluated here, but it is know that the up-scaling of this technology can decrease the modification costs.

Therefore, it is expected that the fiber modification leads to several advantages that will permit optimizations of the fiber-cement formulations (*e.g.* reduction of cement or synthetic fiber contents) and reduction of production costs. Concomitantly, it is expected that composite of fiber-cement of the modified fiber (MF) have mechanical and physical properties and durability that are compatible or better than those reported in other works (Tonoli *et al.* 2009, 2013a,b; Mendes *et al.* 2015; Silva *et al.* 2017)

The Effect of Fibers at Initial Cement Hydration

In this stage of the study, the evaluation of the effect of fiber modification on the initial hydration of the composites was tested in two parts. In part 1, the composite matrix was composed exclusively of Portland cement and in part 2, the composite matrix was composed of Portland cement, limestone, and additives, as described in Table 1. The purpose of the two parts was to ascertain in addition to the effect of the fibers (UMF and MF), the effect of the two matrix formulations on the initial hydration of the fiber-cement composites. Figure 5 shows the evolution of temperature during the initial hydration (0 h to 21 h) of the fiber-cement composites reinforced with UMF and MF without the presence of limestone and additives.

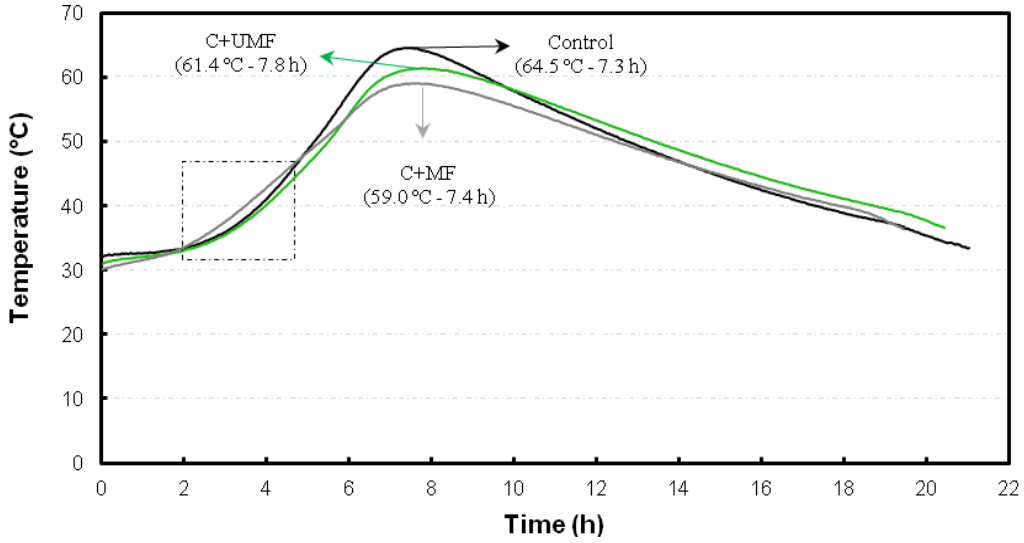

Fig. 5. Evolution of the temperature of the initial hydration along the time for UMF and MF with Portland cement (C), part 1

Figure 5 shows the time that each mixture took to reach the maximum initial hydration temperature. The curves were similar for the different evaluated mixtures. This similarity indicated that UMF and MF did not negatively interfere on the initial hydration of the cement matrix (without the presence of limestone and additives) even though the maximum temperatures and the times to reach this temperature were slightly different.

Lignocellulosic materials contain many inhibitory substances to cement hydration (*e.g.*, hemicelluloses, starches, sugars, phenols, hydroxylated carboxylic acids, *etc.*) with emphasis on low molecular weight carbohydrates and hemicelluloses (Fan *et al*. 2012). However, most of these substances were removed in kraft pulping and bleaching processes. For this reason, the UMF and MF did not cause significant interferences in the initial hydration of the cement in this first part of the evaluation. However, the curve representing

the sample with MF showed a slight increase of temperature in the time interval between 2 h and 5 h (highlighted in Fig. 5), in relation to the control and samples with UMF. The MF reached the lowest maximum temperature (59 °C) in relation to the control and UMF samples (64.5 °C and 61.4 °C, respectively). Another interesting aspect is that the order of the curves in relation to temperature was changed only in the interval of 2 h to 6 h, coinciding with the theoretical hardening period of the hydrated cement pastes. Such behavior may have been associated with reactions between the nano-silica present on the surface of the modified fibers and the cement matrix at the initial stage of hydration. Nano-silica is a highly reactive pozzolanic material and reacts with calcium hydroxide (CH) from cement hydration to form calcium silicate hydrates (CSH) (Zhang and Islam 2012). Concomitantly, the slight increase in the initial hydration temperature of the composite with MF in the period between 2 h and 5 h could have been related to the accelerated hydration of C_3S (tricalcium silicate). Amorphous silica accelerates the hydration rate of C_3S and this acceleration can be explained by assuming that silica lowered the calcium- and hydroxyl-ion concentrations during the first minutes of hydration, increasing the conversion rate of a first protective hydrate layer into another less protective layer (Stein and Stevels 1964).

In contrast, the evolution of hydration temperature of the samples whose matrices were composed of cement, limestone, and additives (C_{LA}, Fig. 6, part 2) was completely different, except for the control curve (composed only of cement).

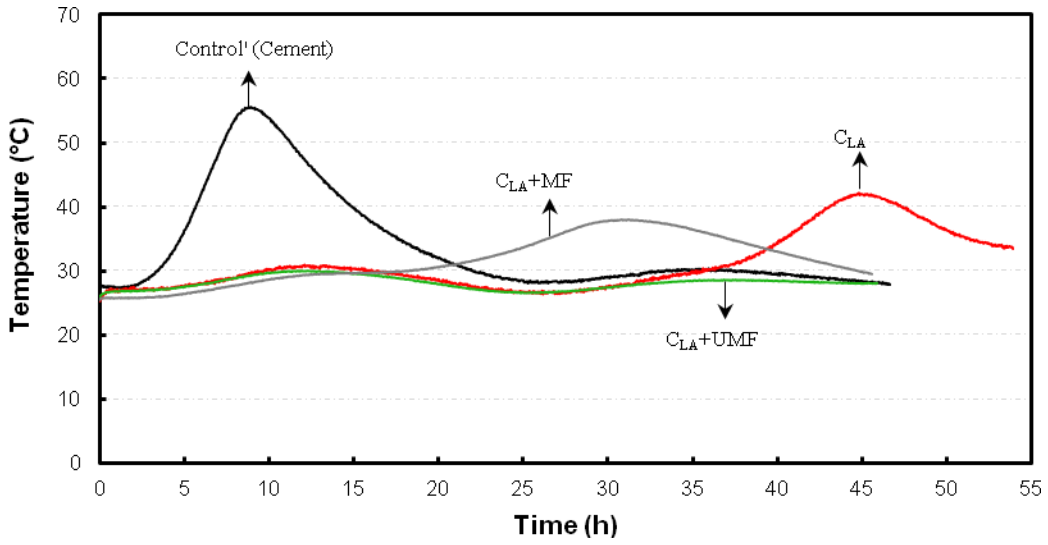

Fig. 6. Evolution of the temperature of the initial hydration along the time for part 2: Control' = Cement; C_{LA} = Cement + Limestone + Additives; C_{LA}+UMF = Cement + Limestone + Additives + Unmodified Fiber; and C_{LA}+MF = Cement + Limestone + Additives + Modified Fiber

The sample containing UMF did not show temperature elevation during the increase of time of hydration. In addition, it was evident that the presence of MF influenced the anticipation of temperature elevation when compared to C_{LA} (cement, limestone, and additions) and C_{LA} + UMF (cement, limestone, and additions + unmodified fiber). However, when the control sample was compared to other samples evaluated in part 2, there was a considerable delay and low temperature elevation for C_{LA} + MF and C_{LA}, as well as the lack of heat emission for C_{LA} + UMF (Table 5).

Table 5. Mean Values of the Maximum Temperature (*T* max), Time to Reach the Maximum Temperature (*t* max), and the Inhibition Index (*II*) of the Different Formulations Evaluated in the Initial Hydration Period (Part 1 and 2)

Formulations		*T* max (ºC)	*t* max (h)	*II* (%)
Part 1	Control	64.5 ± 0.1	7.3 ± 0,6	-
	C + UMF	61.4 ± 1.2	7.8 ± 0.2	0.1 ± 0.1
	C + MF	59.1 ± 0.2	7.4 ± 0.4	-0.1 ± 0.2
Part 2	Control'	56.0 ± 2.2	8.8 ± 0.5	-
	C_{LA}	42.4 ± 0.5	44.8 ± 0.7	67.1 ± 4.8
	C_{LA} + UMF	29.0 ± 0.8	39.0 ± 6.4	179.2 ± 32.2
	C_{LA} + MF	38.6 ± 0.3	30.7 ± 2.0	53.8 ± 5.9
Control and Control ' = hydrated cement for the tests of Figs. 4 and 5, respectively; C = cement; UMF = unmodified fibers; MF = modified fibers; L = limestone; A = additives				

The results of Table 5 showed that a higher temperature (*T* max) and lower time (*t* max) to reach this temperature resulted in lower inhibition indexes (*II*). The *II* for the samples from part 1 were close to zero and revealed that UMF and MF showed low inhibition. In contrast, in the tests of part 2 it was revealed that the *II* of the UMF and MF mixtures presented values higher than 50 and can be classified as excessive inhibition and high inhibition, respectively (Table 1), according to the classification proposed by Okino *et al*. (2004). The higher water content (water:cement ratio = 1) used in the mixture and the presence of limestone and additives (HPMC and ADVA) may have influenced the behavior of the temperature curves of the initial hydration of the evaluated mixtures in part 2 (Fig. 6). Moreover, some considerations are needed to better understand this behavior. The need to considerably increase the water:matrix ratio (from 0.45 to 0.68) and water:cement ratio (from 0.45 to 1) when the fibers and other components (limestone and additives) were added was justified by the incorporation of fibers having hydrophilic characteristics (UMF and MF). Furthermore, limestone (30%) turn difficult the fluidity of the composite mixture, especially when handling small quantities. The release of the heat of hydration can undergo changes as a function the mix proportioning parameters including water content, limestone volume, and water-to-cement (W/C) (Ng *et al*. 2017). The degree of hydration and volume of hydrated products are also influenced by the water:cement and limestone:cement ratios (Bonavetti *et al.* 2003). However, little or nothing was known about the maximum limit of water:cement and water:cement:limestone ratio, which may have negatively interfered with the initial hydration heat of the cement-based pastes.

According to recent literature, the addition of limestone to cement as a partial substitute (filler) favors the initial hydration reactions of the cement by providing more nucleation sites for the formation of hydration products (Bentz *et al*. 2017; Moon *et al.* 2017). Limestone is used, as an inert filler in concrete to reduce the cement consumption, reduce the heat generation during hardening and promote the sustainability of concrete construction (Ng *et al.* 2017). In general, the influence of limestone on the heat of hydration can be observed at early ages (up to 48 h), which is usually attributed to dilution or nucleation effects. The influence of limestone on the heat of hydration is much less significant at later ages (Tennis *et al*. 2011).

Hydroxypropyl methylcellulose is already an organic polymer derived from cellulose and is soluble in water. Its addition to cement mixtures leads to the increase of plasticity, cohesion, workability, and water retention of the hydrated cement (Pourchez *et*

al. 2006). Additionally, HPMC can significantly delay the hydration induction period and acceleration period of cement pastes (Pourchez *et al*. 2006), mainly due to their influences on C_3S dissolution, C-S-H nucleation-growth process, and portlandite precipitation (Pourchez *et al.* 2010). Qu and Zhao (2017) observed that HPMC can reduce the hydration exothermic rate peak between 5 h and 20 h, and that the existence of O–H groups enables HPMC to chemically combine with Ca^{2+}, decreasing Ca^{2+} concentration in the cement pastes, finally leading to a retardation effect on hydration at early ages. Additionally, the ADVA, a superplasticizer additive (surfactant) based on polycarboxylates, has a high potential to reduce water demand. Surfactants can be adsorbed on the surface of the cement and hydrate clinker and change the surface properties of the cement paste (Merlin *et al*. 2005), causing improvement in particle dispersion and paste flow (Yoon and Kim 2018). Palacios *et al.* (2009) also reported the retarding effect from addition of polycarboxylate superplasticizer and its adsorption on the hydration of cement pastes. It has been well accepted that the retarding effects of superplasticizers are related to the amount of their adsorption on the surface of the cement grains. A higher amount of adsorption generally results in a stronger retarding effect on cement hydration (Zhang and Kong 2015). Thus, these effects depend on the molecular architecture of the sulfate and on the additives dosage (Nawa 2006; Houst *et al.* 2008). The composition of the phase and the microstructure of the cement hydration product can also be influenced by the polycarboxylate superplasticizer (Feng *et al.* 2018).

Finally, the delay and the reduction of the exothermic heat of the initial hydration and the increase of the inhibition index, observed in Fig. 6 and Table 5, was attributed to the almost null reactivity of the limestone (calcium carbonate), which contributes to the reduction of the heat of the hydration, since it replaces cement and does not react with water; the presence of additives with hydration retarding properties, even in small proportions; and the increase in the water: cement ratio of 0.68: 1 to 1: 1, due to the partial replacement of the cement, hinders the exothermic heat generation and delays the initial hydration of the cement.

CONCLUSIONS

1. The surface modification of the cellulose pulp fibers applied in this study showed that the MF presented a homogeneous surface coating formed by spherical nano-silica. The CI of the fibers was reduced approximately 15% and the specific surface area, volume, and pore diameter increased from 2.3 m^2/g to 7.1 m^2/g (209% increase), from 0.011 cm^3/g to 0.025 cm^3/g (134% increase), and from 33.6 Å to 37.1 Å (10% increase), respectively, after fiber modification.
2. The nano-silica on the surface of MF did not inhibit the hydration of the cement paste (without limestone and additives) and slightly accelerated the hydration process during the period of hardening.
3. The inhibition index of the composites was impaired when limestone (30%) and additives (2%) were added as partial replacement of cement, as well as when the water:cement ratio increased, retarding the initial hydration of the cement. This was attributed to the almost null reactivity of the limestone (calcium carbonate), which does not contribute to the heat of hydration.

ACKNOWLEDGMENTS

The authors are grateful for the support of the Reference Center for Nature Conservation and Recovery of Degraded Area (CRAD), and the financial support of the Foundation for Research Support of the Federal District (FAPDF), Foundation for Research Support of Minas Gerais (FAPEMIG), National Council for Scientific and Technological Development (CNPq), and the Coordination of Improvement of Higher Education Personnel (CAPES).

REFERENCES CITED

ABNT NBR 5737 (1992). "Sulphate resistant Portland cements," Brazilian Association of Technical Standards, Rio de Janeiro, Brazil.

Agopyan, V., Savastano, Jr., H., John, V. M., and Cincotto, M. A. (2005). "Developments on vegetable fibre–cement based materials in São Paulo, Brazil: An overview," *Cement & Concrete Composites* 27(5), 527-536. DOI: 10.1016/j.cemconcomp.2004.09.004

Ardanuy, M., Claramunt, J., and Toledo Filho, R.D. (2015). "Cellulosic fiber reinforced cement-based composites: A review of recent research," *Construction and Building Materials* 79, 115-128. DOI: 10.1016/j.conbuildmat.2015.01.035

Ashori, A., Sheyhnazari, S., Tabarsa, T., Shakeri, A., and Golalipour, M. (2012). "Bacterial cellulose/sílica nanocomposites: Preparation and characterization," *Carbohydrate Polymers* 90(1), 413-418. DOI: 10.1016/j.carbpol.2012.05.060

Belgacem, M. N., and Gandini, A. (2005). "The surface modification of cellulose fibres for use as reinforcing elements in composite materials," *Composite Interfaces* 12(1-2), 41-75. DOI: 10.1163/1568554053542188

Bentz, D. P., Ferraris, C. F., Jones, S. Z., Lootens, D., and Zunino, F. (2017). "Limestone and silica powder replacements for cement: Early-age performance," *Cement and Concrete Composites* 78, 43-56. DOI: 10.1016/j.cemconcomp.2017.01.001

Benvenutti, E. V., Moro, C. C., Costa, T. M. H., and Gallas, M. R. (2009). "Materiais híbridos à base de sílica obtidos pelo método sol-gel [Silica-based hybrid materials obtained by the sol-gel method]," *Química Nova* 32(7), 1926-1933.

Besbes, I., Vilar, M. R., and Boufi, S. (2011). "Nanofibrillated cellulose from TEMPO oxidized eucalyptus fibres: Effect of the carboxyl content," *Carbohydrate Polymers* 84(3), 975-983. DOI: 10.1016/j.carbpol.2010.12.052

Bezerra, E. M., Joaquim, A. P., Savastano, Jr., H., John, V. M., and Agopyan, V. (2006). "The effect of different mineral additions and synthetic fiber contents on properties of cement based composites," *Cement and Concrete Composites* 28(6), 555-563. DOI: 10.1016/j.cemconcomp.2006.02.001

Bilba, K., and Arsene, M. A. (2008). "Silane treatment of bagasse fiber for reinforcement of cementitious composites," *Composites Part A* 39, 1488-1495. DOI: 10.1016/j.compositesa.2008.05.013

Bonavetti, V., Donza, H., Menendez, G., Cabrera, O., and Irassar, E. F. (2003). "Limestone filler cement in low w/c concrete: A rational use of energy," *Cement and Concrete Research* 33(6), 865-871. DOI: 10.1016/S0008-8846(02)01087-6

Brumaud, C., Bessaies-Bey, H., Mohler, C., Baumann, R., Schmitz, R., and Roussela, N. (2013). "Cellulose ethers and water retention," *Cement and Concrete Research* 53, 176-184. DOI: 10.1016/j.cemconres.2013.06.010

Cao, Y., and Tan, H. (2005). "Study on crystal structures of enzyme-hydrolyzed cellulosic materials by X-ray diffraction," *Enzyme and Microbial Technology* 36(2-3), 314-317. DOI: 10.1016/j.enzmictec.2004.09.002

Cessa, R. M. A., Celi, L., Vitorino, A. C. T., Novelino, J. O., and Barberis, E. (2009). "Área superficial específica, porosidade da fração argila e adsorção de fósforo em dois latossolos vermelhos [Specific surface area, porosity of the clay fraction and adsorption of phosphorus in two red latosols]," *Revista Brasileira de Ciências do Solo* 33(5), 1153-1162.

Fan, M., Ndikontar, M. K., Zhou, X., and Ngamveng, J. N. (2012). "Cement-bonded composites made from tropical woods: Compatibility of wood and cement," *Construction and Building Materials* 36, 135-140. DOI: 10.1016/j.conbuildmat.2012.04.089

Farias, W. M. (2012). *Evolutionary Processes of Chemical Weathering and its Action on the Hydromechanical Behavior of Soils of the Central Plateau*, Ph.D. Thesis, University of Brasília, Brasília, Federal District, Brazil.

Feng, W., Xu, J., Chen, P., Jiang, L., Song, Y., and Cao, Y. (2018). "Influence of polycarboxylate superplasticizer on chloride binding in cement paste," *Construction and Building Materials* 158, 847-854. DOI: 10.1016/j.conbuildmat.2017.10.086

Ford, E. N. J., Mendon, S. K., Thames, S. F., and Rawlins, J. W. (2010). "X-ray diffraction of cotton treated with neutralized vegetable oil-based macromolecular crosslinkers," *Journal of Engineered Fibers and Fabrics* 5(1), 10-20.

French, A. D. (2014). "Idealized powder diffraction patterns for cellulose polymorphs," *Cellulose* 21(2), 885-896. DOI: 10.1007/s10570-013-0030-4

Gram, H. E. (1983). *Durability of Natural Fibers in Concrete*, Swedish Cement and Concrete Research Institute, Stockholm.

Hofstrand, A. D., Moslemi, A. A., and Garcia, J. F. (1984). "Curing characteristics of wood particles from nine northern Rocky Mountain species mixed with Portland cement," *Forest Products Journal* 34(2), 57-61.

Houst, Y. F., Bowen, P., Perche, F., Kauppi, A., Borget, P., Galmiche, L., Le Meins, J. F., Lafuma, F., Flatt, R. J., Schober, I., *et al.* (2008). "Design and function of novel superplasticizers for more durable high performance concrete (superplast project)," *Cement and Concrete Research* 38(10), 1197-1209. DOI: 10.1016/j.cemconres.2008.04.007

Hussain, A. Calabria-Holleya, J., Schorr, D., Jianga, Y., Lawrence, and M., Blanchet, P. (2018). "Hydrophobicity of hemp shiv treated with sol-gel coatings," *Applied Surface Science* 434, 850-860. DOI: 10.1016/j.apsusc.2017.10.210

Iftekhar, S., Srivastava, V., and Sillanpää, M. (2017). "Enrichment of lanthanides in aqueous system by cellulose based silica nanocomposite," *Chemical Engineering Journal* 320, 151-159. DOI: 10.1016/j.cej.2017.03.051

Khan, M. I., Abbas, Y. M., and Fares, G. (2017). "Review of high and ultrahigh performance cementitious composites," *Journal of King Saud University – Engineering Sciences* 29, 339-347. DOI: 10.1016/j.jksues.2017.03.006

Klemm, D., Heublein, B., Fink, H. P., and Bohn, A. (2005). "Cellulose: Fascinating biopolymer and sustainable raw material," *Angewandte Chemie-International Edition* 44(22), 3358-3393. DOI: 10.1002/anie.200460587

Lowell, S., and Shields, J. E. (1991). *Powder Surface Area and Porosity*, 3rd Edition, Chapman & Hall, London, England.

Mendes, R. F., Mendes, L. M., Oliveira, J. E. d., Savastano Jr., H., Glenn, G., and Tonoli, G. H. D. (2015). "Modification of eucalyptus pulp fiber using silane coupling agents with aliphatic side chains of different length," *Polymer Engineering and Science* 55, 1273-1280. DOI: 10.1002/pen.24065

Merlin, F., Guitouni, H., Mouhoubi, H., Mariot, S., Vallée, F., and Van Damme, H. (2005). "Adsorption and heterocoagulation of nonionic surfactants and latex particles on cement hydrates," *Journal Colloid Interface Science* 281(1), 1-10. DOI: 10.1016/j.jcis.2004.08.042

Moon, G. D., Oh, S., Jung, S. H., and Choi, Y. C. (2017). "Effects of the fineness of limestone powder and cement on the hydration and strength development of PLC concrete," *Construction and Building Materials* 135, 129-136. DOI: 10.1016/j.conbuildmat.2016.12.189

Nawa, T. (2006). "Effect of chemical structure on steric stabilization of polycarboxylate based superplasticizer," *Journal of Advanced Concrete Technology* 4(2), 225-232. DOI: 10.3151/jact.4.225

Ng, P. L., Chenc, J. J., and Kwan, A. K. H. (2017). "Adiabatic temperature rise of concrete with limestone fines added as a filler," *Procedia Engineering* 172, 768-775. DOI: 10.1016/j.proeng.2017.02.121

Okino, E. Y. A., Souza, M. R. S., Santana, M. A. E., Sousa, M. E., and Teixeira, D. E. (2004). "Chapa aglomerada de cimento-madeira de *Hevea brasiliensis* mull. arg. [Agglomerated cement-wood sheet *Hevea brasiliensis* mull. arg.]," *Árvore* 28(3), 451-457.

Onuaguluchi, O., and Banthia, N. (2016). "Plant-based natural fibre reinforced cement composites: A review," *Cement and Concrete Composites* 68, 96-108. DOI: 10.1016/j.cemconcomp.2016.02.014

Palacios, M., Puertas, F., Bowen, P., and Houst, Y. F. (2009). "Effect of PCs superplasticizers on the rheological properties and hydration process of slag-blended cement pastes," *Journal of Materials Science* 44(10), 2714-2723. DOI: 10.1007/s10853-009-3356-4

Pehanich, J. L., Blankenhorn, P. R., Silsbee, M. R. (2004). "Wood fiber surface treatment level effects on selected mechanical properties of wood fiber–cement composites," *Cement and Concrete Research* 34(1), 59-65. DOI: 10.1016/S0008-8846(03)00193-5

Pena, E. Q., Vieira, C. B., Silva, C. A., Seshadri, V., and Araújo, F. G. S. (2008). "Caracterização dos parâmetros de porosidade de concentrados de minérios de ferro pelo método de adsorção de nitrogênio [Characterization of the porosity parameters of iron ore concentrates by the nitrogen adsorption method]," *Tecnologia em Metalurgia e Materiais* 4(4), 53-57. DOI: 10.4322/tmm.00404010

Pinto, R. J. B., Marques, P. A. A. P., Barros-Timmons, A. M. B., Trindade, T., and Pascoal Neto, C. (2008). "Novel SiO_2/cellulose nanocomposite obtained by *in situ* synthesis and *via* polyelectrolytes assembly," *Composites Science and Technology* 68(3-4), 1088-1093. DOI: 10.1016/j.compscitech.2007.03.001

Pizzol, V. D., Mendes, L. M., Frezzatti, L., Savastano Jr., H., and Tonoli, G.H.D. (2014). "Effect of accelerated carbonation on the microstructure and physical properties of hybrid fiber-cement composites," *Minerals Engineering* 59, 101-106. DOI: 10.1016/j.mineng.2013.11.007

Pourchez, J., Grosseau, P., and Ruot, B. (2010). "Changes in C_3S hydration in the presence of cellulose ethers," *Cement and Concrete Research* 40(2), 179-188. DOI: 10.1016/j.cemconres.2009.10.008

Pourchez, J., Peschard, A., Grosseau, P., Guyonnet, R., Guilhot, B., and Valle´e, F. (2006). "HPMC and HEMC influence on cement hydration," *Cement and Concrete Research* 36(2), 288-294. DOI: 10.1016/j.cemconres.2005.08.003

Qu, X., and Zhao, X. (2017). "Influence of SBR latex and HPMC on the cement hydration at early age," *Case Studies in Construction Materials* 6, 213-218. DOI: 10.1016/j.cscm.2017.04.006

Raabe, J., Fonseca, A. S., Bufalino, F., Ribeiro, C., Martins, M. A., Marconcine, J. M., and Tonoli, G. H. D. (2015). "Biocomposite of cassava starch reinforced with cellulose pulp fibers with deposition of sílica (SiO_2) nanoparticles," *Journal of Nanomaterials* 2015, Article ID 493439, 1-9. DOI: 10.1155/2015/493439

Raabe, J., Fonseca, A. S., Bufalino, L., Ribeiro, C., Martins, M. A., Marconcine, J. M., and Tonoli, G. H. D. (2014). "Evaluation of reaction factors for deposition of sílica (SiO_2) nanoparticles on cellulose fibers," *Carbohydrate Polymers* 114, 424-431. DOI: 10.1016/j.carbpol.2014.08.042

Santana, M. F. S., Katekawa, M. E., Tannous, K., Lima, A. K. V. O., and Gasparetto, C. A. (2012). "Área superficial e porosidade da fibra alimentar do albedo de laranja," *Revista Brasileira de Produtos Agroindustriais* 14(3), 261-273.

Santos, S. F., Tonoli, G. H. D., Mejia, J. E. B., Fiorelli, J., and Savastano, Jr., H. (2015). "Non-conventional cement based composites reinforced with vegetable fibers: A review of strategies to improve durability," *Materiales de Construcción* 65(317), 1-14. DOI: 10.3989/mc.2015.05514

Silva, F. d. A., Chawla, N., and Filho, R. D. d. T. (2008). "Tensile behavior of high performance natural (sisal) fibers," *Composites Science and Technology* 68 (15-16), 3438-3443. DOI: 10.1016/j.compscitech.2008.10.001

Silva, E. J., Marques, M. L., Velasco, F. G., Fornari Jr., C., Luzardo, F. M., and Tashima, M. M. (2017). "A new treatment for coconut fibers to improve the properties of cementbased composites – Combined effect of natural latex/pozzolanic materials," *Sustainable Materials and Technologies* 12, 44-51. DOI: 10.1016/j.susmat.2017.04.003

Sing, K. S. W., Everett, D. H., Haul, R. A. W., Moscou, L., Pierotti, R. A., Rouquerol, J., and Siemieniewska, T. (1985). "Reporting physisorption data for gas/solid systems with special reference to the determination of surface area and porosity," *Pure and Applied Chemistry* 57(4), 603-619. DOI: 10.1351/pac198557040603

Singh, S. M. (1985). "Alkali resistance of some vegetable fibers and their adhesion with Portland cement," *Res. Ind.* 15, 121-126.

Singh, L. P., Bhattacharyya, S. K., Kumar, R., Mishra, G., Sharma, U., Singh, G., Ahalawat, S. (2014). "Sol-Gel processing of silica nanoparticles and their applications," *Advances in Colloid and Interface Science* 214, 17-37. DOI: 10.1016/j.cis.2014.10.007

Soufeiani, L., Raman, S. N., Jumaat, M. Z. B., Alengaram, U. J., Ghadyani, G., and Mendis, P. (2016). "Influences of the volume fraction and shape of steel fibers on fiber-reinforced concrete subjected to dynamic loading – A review," *Engineering Structures* 124, 405-417. DOI: 10.1016/j.engstruct.2016.06.029

Stein, H. N., and Stevels, J. M. (1964). "Influence of silica on the hydration of 3CaO, SiO_2," *Journal of Applied Chemistry* 14(8), 338-346. DOI: 10.1002/jctb.5010140805

Svarovsky, L. (1987). *Powder Testing Guide Methods of Measuring the Physical Properties of Bulk Powders*, British Materials Handling Board, London, England.

Tennis, P. D., Thomas, M. D. A., and Weiss, W. J. (2011) *State-of-the-Art Report on Use of Limestone in Cements at Levels of up to 15%* (SN3148), Portland Cement Association, Skokie, IL, USA.

Tolêdo Filho, R. D., Scrivener, K., England, G. L., and Ghavami, K. (2000). "Durability of alkali-sensitive sisal and coconut fibres in cement mortar composites," *Cement and Concrete Composites* 22(2), 127-143. DOI: 10.1016/S0958-9465(99)00039-6

Tonoli, G. H. D., Rodrigues Filho, U. P., Savastano, Jr., H., Bras, J., Belgacem, M. N., and Rocco Lahr, F. A. (2009). "Cellulose modified fibres in cement based composites," *Composites Part A: Applied Science and Manufacturing* 40(12), 2046-2053. DOI: 10.1016/j.compositesa.2009.09.016

Tonoli, G. H. D., Belgacem, M. N., Siqueira, G., Bras, J., Savastano Jr, H., and Rocco Lahr, F. A. (2013a). "Processing and dimensional changes of cement based composites reinforced with surface-treated cellulose fibres," *Cement & Concrete Composites* 37, 68-75. DOI: 10.1016/j.cemconcomp.2012.12.004

Tonoli, G. H. D., Mendes, R. F., Siqueira, G., Bras, J., Belgacem, M. N., and Savastano Jr, H. (2013b). "Isocyanate-treated cellulose pulp and its effect on the alkali resistance and performance of fiber cement composites," *Holzforschung* 67, 1-9. DOI: 10.1515/hf-2012-0195

Tonoli, G. H. D., Pizzol, V. D., Urea, G., Santos, S. F., Mendes, L. M., Santos, V., John, V. M., Frias, M., and Savastano Jr., H. (2016). "Rationalizing the impact of aging on fiber-matrix interface and stability of cement-based composites submitted to carbonation at early ages," *Journal of Materials Science* 51(17), 7929-7943. DOI: 10.1007/s10853-016-0060-z

Weatherwax, R. C., and Tarkow, H. (1964). "Effect of wood on setting of Portland cement," *Forest Products Journal* 14, 567-570.

Wei, J., and Meyer, C. (2015). "Degradation mechanisms of natural fiber in the matrix of cement composites," *Cement and Concrete Research* 73, 1-16. DOI: 10.1016/j.cemconres.2015.02.019

Wei, J., and Meyer, C. (2017). "Degradation of natural fiber in ternary blended cement composites containing metakaolin and montmorillonite," *Corrosion Science* 120, 42-60. DOI: 10.1016/j.corsci.2016.12.004

Wei, J. (2018). "Degradation behavior and kinetics of sisal fiber in pore solutions of sustainable cementitious composite containing metakaolin," *Polymer Degradation and Stability* 150, 1-12. DOI: 10.1016/j.polymdegradstab.2018.01.027

Xie, K., Yu, Y., and Shi, Y. (2009). "Synthesis and characterization of cellulose/silica hybrid materials with chemical crosslinking," *Carbohydrate Polymers* 78(4), 799-805. DOI: 10.1016/j.carbpol.2009.06.019

Yoon, J. Y., and Kim, J. H. (2018). "Evaluation on the consumption and performance of polycarboxylates in cement-based materials," *Construction and Building Materials* 158, 423-431. DOI: 10.1016/j.conbuildmat.2017.10.004

Zhang, M., and Islam, J. (2012). "Use of nano-silica to reduce setting time and increase early strength of concretes with high volumes of fly ash or slag," *Construction and Building Materials* 29, 573-580. DOI: 10.1016/j.conbuildmat.2011.11.013

Zhang, Y., and Kong, X. (2015). "Correlations of the dispersing capability of NSF and PCE types of superplasticizer and their impacts on cement hydration with the

adsorption in fresh cement pastes," *Cement and Concrete Research* 69, 1-9. DOI: 10.1016/j.cemconres.2014.11.009

Zhang, Y., Kong, X., Lu, Z., Lu, Z, and Hou, S. (2015). "Effects of the charge characteristics of polycarboxylate superplasticizers on the adsorption and the retardation in cement pastes," *Cement and Concrete Research* 67, 184-196. DOI: 10.1016/j.cemconres.2014.10.004

Article submitted: November 16, 2017; Peer review completed: February 16, 2018; Revised version received: March 19, 2018; Accepted: March 20, 2018; Published: March 22, 2018.
DOI: 10.15376/biores.13.2.3525-3544